COMPUTER-AIDED DESIGN & APPLICATIONS, 2018
VOL. 15, NO. 3, 416–431
https://doi.org/10.1080/16864360.2017.1397892

A proposal of experimental protocol to assembly scanning

Pablo Coves [a], Jean-Claude Léon [a], Damien Rohmer [a] and Raphael Marc [b]

[a]Grenoble University, LJK laboratory, Inria team IMAGINE; [b]EDF Lab, France

ABSTRACT

Acquisition of 3D objects using laser scans has become rather common. Most of the time in mechanical engineering, scanning processes are dedicated to standalone components, as part of a reverse engineering pipeline. Though a product, i.e., a set of assembled components, can also be laser scanned, such a scan has no real interest if the objective is to reverse engineer the whole set of assembly components because of the occluded areas generated by components through their contact areas. Indeed, several scans, with some dismounted components, are mandatory to reduce occlusions. Consequently, how many components should be removed? Into which extent is it possible to obtain a good coverage of each component? How many different assembly configurations should be required to obtain enough information? All these meaningful questions can be addressed under the umbrella of the setting of a scanning protocol. This is the proposal described here where a protocol is described and tested that aims at producing the input of a reverse engineering process devoted to CAD assembly reconstruction.

KEYWORDS

3D scanners; Rapid Prototyping; Assembly; Reverse engineering; Metrology; 3D printing

1. Introduction

Scanning standalone components has become a routine task for many people though there may be some issues regarding the selection of the scanner with regard to the dimension of the object or the dimensions of the area of terrain and the accuracy of the measures. Depending on the use of the scanned data, the information extracted from these scanned data, it can be worth formalizing the acquisition phase through a protocol [2, 3, 7, 10].

Here, the emphasis is placed on scanning mechanical assemblies to produce data used as input of a reverse engineering process aiming at generating a CAD assembly model. This CAD model should cover the largest possible extent of the real assembly and it should be consistent, i.e., the digital model of the assembly should be comparable to those produced directly from CAD software using mating constraints between components, ... Obviously, this objective cannot be achieved solely using a digitized representation of the real assembled components because a laser scan would face many occluded areas, leaving the reverse engineering process with impossibilities to reconstruct large areas, even entire components. Indeed, the acquisition of an assembly requires the combination of an assembly or disassembly process interacting with scanning processes. Such a combination adds complexity to the scanning processes due to the number of components being processed and the information looked for regarding the interfaces between components. Also, the morphology of components add several issues, e.g., whether they are thin or not compared to the accuracy of the scanner, because there is a need to scan as many components as possible and, possibly, all of them. Reducing the scanning process to the scans of individual components does not ensure the compatibility of the dimensions of their digital counterparts, as pointed out by Langbein *et al.* [8] who applied the concept of beautification to dimensions so that they reflect the nominal values currently used in digital mock-ups. They also addressed the case of geometric properties, e.g., parallelism, orthogonality, required to be able to produce what could be referred to as consistent solid models that can be used as assembly constraints. More recently, Monszpart *et al.* showed the efficiency of integrating some of these geometric constraints within RANSAC based primitive extractions [11].

Consequently, the purpose of the paper is a first formalization of an experimental protocol of assembly scanning processes that can improve the quality and efficiency of these processes. The efficiency refers to the number of dismounting/mounting operations and associated scans that are required to cover, as much as possible, the surfaces of the components to improve the reverse engineering process. The quality refers to the accuracy of the

CONTACT Pablo Coves Pablo.Coves@inria.fr; Jean-Claude Léon Jean-Claude.Leon@grenoble-inp.fr; Damien Rohmer Damien.Rohmer@inria.fr; Raphael Marc Raphael.Marc@edf.fr

measures across the whole protocol and the fidelity of the reverse engineered assembly compared to the real one.

Digitizing an assembly with a laser scan technology is not the only possibility, one could think using CT scanners devoted to industrial components [1, 7]. This technology offers the capability to digitize an assembly in an assembled configuration, at once in principle. CT scans are often used for non-destructive testing. They can be used to scan assemblies as metrology for manufacturing, checking dimensions and clearances. Resolution and assembly size, however, are coupled to determine whether an assembly can be candidate to such a technology. On the one hand, large assemblies like equipment in power plants are out of range of this technology. In the context of EDF company, this technology is not adapted because of the size of the equipment that can reach several meters size. On the other hand, CT scanners face also difficulties to produce satisfactory results when an assembly contains materials with significantly different densities or when components of same constitutive material share an interface, i.e., a contact area, because this interface hardly appears in a CT scan.

The description of the proposed contribution is organized as follows. Section 2 reviews prior work regarding digitization protocols as well as assembly models. Section 3 introduces the objectives and hypotheses of the proposed study. Section 4 describes the main concepts related to the protocol, its main criteria and their connection with assembly or disassembly processes. Section 5 introduces test assemblies supporting the proposed protocol and synthesizes the key features of the proposed scanning protocol and Section 6 concludes.

2. Related works

Most of the time, laser scanning associated with a reverse engineering process is devoted to standalone components to generate a digital model from its physical counterpart. Indeed, the digital model is a CAD model, often a solid model. Using a laser scanner, an important objective is the largest possible coverage of the object surfaces [2]. To this end, multiple range scans are mandatory to avoid, as much as possible, occluded areas. Consequently, a registration process must take place to reference all the range scans in the same reference frame. Such a process can become time consuming if it must be applied to multiple components of an assembly. Additionally, the registration process increases the overall deviation of the scanned points ε_1 with respect to the real object because it incorporates an ICP-based algorithm [19] referring to a threshold parameter $\varepsilon_2 > \varepsilon_1$.

Up to the knowledge of the authors, there has been no prior work specifically focusing on issues about the laser scanning process of assemblies. Laser scan protocols have been studied either for standalone manufactured or hand crafted objects [2, 15] or for terrain areas [7, 10], only. CT scan protocols have been developed for the acquisition of moving morphology [3] showing the interest of figuring out a procedure to acquire a new range of digitized data. Likewise Yan *et al.* [18] use a dynamic acquisition principle incorporating trajectories of moving parts of a scene to improve the acquisition of otherwise occluded areas. However, this approach requires a fair amount of data to characterize the trajectory of moving parts. More recently Li *et al.* [9] focused on the detection of joints in digitally acquired mechanisms using a RANSAC based approach. If the amount of digitized data is reduced compared to [18], it is still large compared to poses strictly representing key positions of the assembly and the accuracy of the joint detection is low with an order of few millimeters compared to the accuracy of hand-held laser scans reaching few 0.01 mm.

Because assemblies are under focus and their scanning process involves some mounting or dismounting operations, it is also important to review some work regarding assembly simulation, and assemblies in the large, which can highlight some criteria of interest. Among the basic concepts developed in assembly simulation, the relative mobility of components is a key one [14, 17]. This mobility is used to characterize the condition of extraction / insertion of a component with respect to others. From the insertion / extraction parameters appear another concept that has been formalized, i.e., the number of hands. During a disassembly operation, this concept indicates, when extracting a component, how many other ones, say m, must be kept into position by the user. Otherwise, the component removed would lead to the simultaneous movements of m components. Often, the purpose of assembly simulation is set on sequencing issues. A sequence indicates the possible chronology of assembly, or disassembly, and can highlight sequential or parallel operations. Also, this is interesting information to structure a sequence of scans.

Additionally, it is important to observe that assembly simulation hardly takes into account the interaction forces between the components during extraction or insertion phases of a component. This is an important point because it can significantly influence a protocol since some operations in a sequence may not be easily achieved, e.g., if two components are linked using a tight fit, and it can also influence some operations because interaction forces may require the use of some tooling equipment.

Based on this review, it is now possible to set the objectives and hypotheses of the proposed contribution.

3. Objectives and hypotheses

The purpose is the digitization of an assembly as an input to a reverse engineering process aimed at producing a digital assembly model of type CAD, i.e., as available through CAD assembly software modules where components share surfaces representing their physical contact areas. The digitizing technique is laser scan. This means, the scanning process should be able to produce enough information so that as many of its components as possible can be reversed engineered as well as their relative positions. Clearly, this can be achieved only if an assembly or disassembly process is associated with scanning processes that remove enough occluding areas of components due to their morphology and their contacts forming internal areas of an assembly. To this end, it is important that the digitization process takes into account the largest range possible of component morphology, i.e., size and shape, since assemblies often contain a large diversity of components.

While maximizing the scanned surfaces of components, it is also important to minimize the number of registrations and, hence, the number of scans in order to save time and reduce the cost and the complexity of the scanning process as well as speeding up the reverse engineering process if the number of registrations is minimized. Overall, this is improving the quality of the resulting assembly model.

The purpose of the digitization and reverse engineering processes stands in the generation of CAD assemblies from 'as built' products. This is an important issue for EDF to support the maintenance process of power plant equipment, the training of technical staff, and reverse engineer components or sub systems to derive CAD models for numerical simulation of physical phenomena, e.g., finite element models for structural analysis or finite volumes for thermo-hydraulic simulations.

Regarding hypotheses, they enumerate as follows:

- The test assemblies are chosen to fit into 27 dm^3, i.e., around 300 mm cubed. This is restrictive compared to the size of power plant equipment where some machinery can reach a reference size of several meters. The component mass should not exceed 5 kg so that all the components can be moved manually without any specific tooling. This is also restrictive compared to power plant machinery where component masses can reach hundreds to thousands kilos;
- The laser scanner used is of hand-held type, e.g., T-Scan, so that the accessibility around an object is maximized and multiple stations around an object can be avoided to maximize the efficiency of the digitization process. More precisely, it is a Leica T-Scan 5 (see Figure 1) with an accuracy of less than 0.05 mm. The T-Scan is consistent with respect to the maximal size of the test assemblies.This is a simplification compared to the LIDAR scan required for large scale objects, i.e., roughly larger than a meter, which is often the case of power plant machinery;
- The constitutive components of an assembly are spread among three categories. The standard components are the first one. It designates the set of components like screws, nuts, . . . , whose dimensions are governed by standardized parameters. They can be found in any type of assembly. The second one contains components that can be identical across products of the same family [16]. They are less frequent than components of the first category and their shape is more complex, usually with free-form surfaces. Their reverse engineering process can hardly be automated. The last category contains the specific components, i.e., components devoted to a given product. Their reverse engineering process is also specific, similarly to the second category.

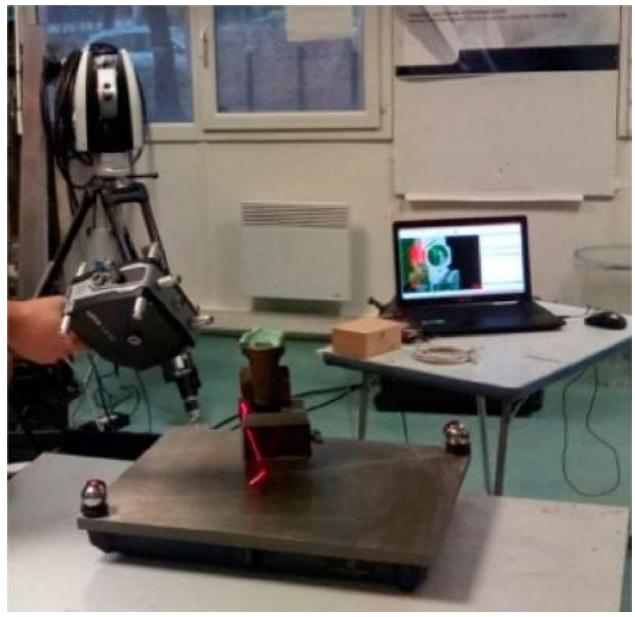

Figure 1. Hand-held laser scanner Leica T-Scan 5 used for scanning test assemblies.

Now, let us describe the proposed protocol reduced to a subset of its major concepts since the diversity of mechanisms cannot be covered entirely. Two test assemblies are used to illustrate these concepts (see Section 5).

4. Scanning protocol

4.1. Major concepts of the scanning protocol

The scanning process of an assembly aims at producing point clouds to reverse engineer this assembly

and produce a CAD assembly model. At this point, it seems important to observe some common denominator of CAD assembly models. First of all, the component dimensions used in CAD are nominal dimensions, i.e., its dimensions are regarded as reference dimensions as if the component could be manufactured perfectly without any distortion. Consequently, the digital model of the component is one among the range of manufactured components whose dimensions fit into the manufacturing tolerances. Commonly, when generating a CAD assembly model, CAD components are '*assembled*', i.e., using geometric constraints like surface mating, coaxial axes, . . . , to prescribe their respective positions. Such a process often ends up producing null clearances in a CAD assembly model, i.e., components are touching each other in the sense that they share common faces (see Figure 2a). Now considering the real components, they are subjected to the inherent inaccuracies of manufacturing processes and their real dimensions reflect the effective clearances between the components. Still in the example of Figure 2, the real diameters of the nut and the shaft must result into a loose fit such that the shaft can rotate inside the nut. Such a difference of diameter may or may not come out from the scanning process depending on the accuracy of the scanner and the reverse engineering process, to the knowledge of the authors, is not currently able to express the corresponding constraints. Consequently, scanning independently each assembly component would require shape adjustments like beautification processes [8] to produce a consistent CAD assembly model. When it comes to axial clearances in assemblies, the same observations can be drawn. Based on this analysis, if reverse engineering an assembly is thought as the independent reverse engineering of its components plus the task of relative positioning of its components, such a protocol does not appear efficient. Where CAD components touch each other in a consistent CAD assembly model, this protocol could produce CAD models of the real components with slightly different dimensions. Tedious remodeling of components to reach dimension adjustments would be needed to produce a consistent CAD assembly since reverse engineering algorithms don't produce parameterized CAD solids. At the opposite, solely scanning subassemblies incorporates occlusions where components are in contact with each other and this may lead to difficulties to segment the point clouds to correctly identify components.

Here, we seek a synergy between the scanning protocol and the reverse engineering process of the assembly to obtain efficiently a consistent CAD assembly model that can be used subsequently, similarly to any CAD assembly strictly generated with CAD software. The major concepts used to define a protocol are as follows:

a. Stability of components or sub-assemblies;
b. Minimize the interactions forces between components during insertion/extraction of components, possibly using dummy components;
c. Minimize the number of registration processes needed taking into account the mobility of the assembly;
d. Select an assembly or disassembly sequence such that the number of hands and the occlusion of components can be minimized;
e. Take advantage of the shape complementarity principle to reduce the extent of occluded areas;
f. Avoid the repetitive scans of identical subsets of components in the assembly;
g. Set up specific processes in accordance with peculiar components morphologies, typically very thin components.

As a first observation, we propose to set a connection between assembly/disassembly processes and the scanning protocol as part of the desired synergy. Now, let us

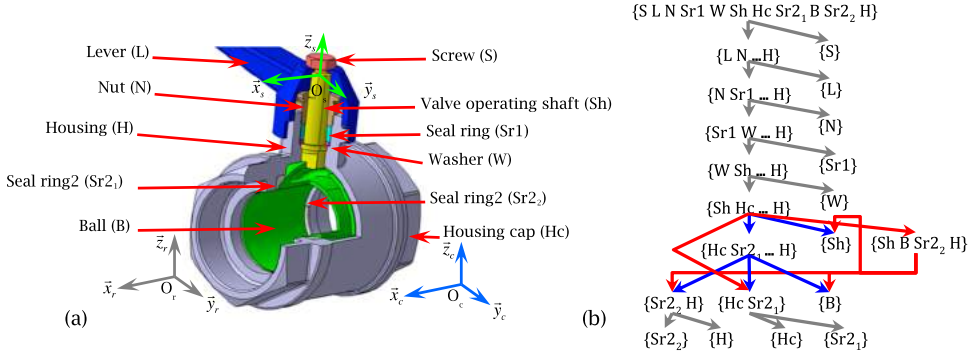

Figure 2. (a) CAD assembly model of a hydraulic gate valve with a partial cut showing internal components. The internal diameter of the nut and the diameter of the shaft are equal and express the contact and rotational movement between these two components. The gray, green, and blue frames are attached to assembly subsets. (b) Possible diassembly sequences with variants (blue and red).

focus on each of these concepts and illustrate them with test configurations.

4.2. Stability of components or sub-assemblies

A first common criterion holds in the stability of the component or sets of assembled components scanned, collectively named C. On the one hand, reference surfaces in metrology are often planar or few planar ones, e.g., a vee. On the other hand, boundary surfaces of C may not be able to exhibit a planar surface or set of surfaces producing a stable contact with a reference plane or any other surface of reference at each step of an assembly or disassembly sequence of the scanning protocol.

The proposed solution to achieve stable positions and enhance the visibility of C is the use of a combination of metrology equipment, e.g., a magnetic vee block, with 'dummy' components, D_C, to hold C and improve its visibility. With respect to visibility, the purpose is to avoid the use, as much as possible, of fixturing devices that reduce the visibility of C with respect to the scanner. Consequently, the use of D_C inserted between the reference surfaces and C ensures the stability of C and improves the scan coverage D_C is designed to satisfy the stability criterion and to ease the segmentation process of the point cloud obtained from C with respect to D_C. To this end, D_C's shape is as simple as possible with a minimum number of planar faces, whenever possible. Because D_C is specific, it is proposed to 3D print them as long as the manufacturing tolerances of these specific components cannot influence the scanner.

As an illustration of D_C, let us consider the test assembly2 (see Figure 14). Given the shape of its housing, the reference surfaces are given by a magnetic vee (see Figure 3a). The stability of the housing is achieved with D_C (see Figure 3c), a 3D printed artifact (see Section 5.2 for a quantitative analysis of manufacturing tolerances).

4.3. Minimize the interaction forces. Dummy components usage

Then, the experimental protocol is influenced by the masses of its components and the fittings between them. As a common denominator between these configurations, it appears important to reduce, as much as possible, all interaction forces during insertions/extractions of components so that the relative movements between components could be operated manually with a low level of interaction force and without complementary tooling. Complementary tooling can become a strong constraint if the equipment needed is not located next to the laser scanner and is rather specific, e.g., a hydraulic press requiring dedicated equipment to perform an assembly or disassembly operation.

Low interaction forces between components ease their manipulations and increase the accuracy of the insertions/extractions, which contributes to lower the number of registrations (see Section 4.4). Monitoring the interaction forces helps simplifying the scanning protocol where the monitoring of some kinematic equivalence classes of components can be removed (see Section 4.4 addressing the mobility of a mechanism).

A proposed solution to lower interaction forces and prohibit the use a specific tooling during the scanning process is the use of dummy components. Here, the purpose of such components is to replace real assembly components with slightly different dimensions, especially to replace tight fits by loose fits and possibly simplify their shapes so that they can be easily and cheaply manufactured. Tests have been performed using 3D printed components.

As an example, the mechanisms analyzed to test the protocol (see Section 5.1) are such that the masses of components range between tens of grams to a couple of kilograms and the fittings are mostly of type loose. Some fittings are rather specific. One appears in the ball

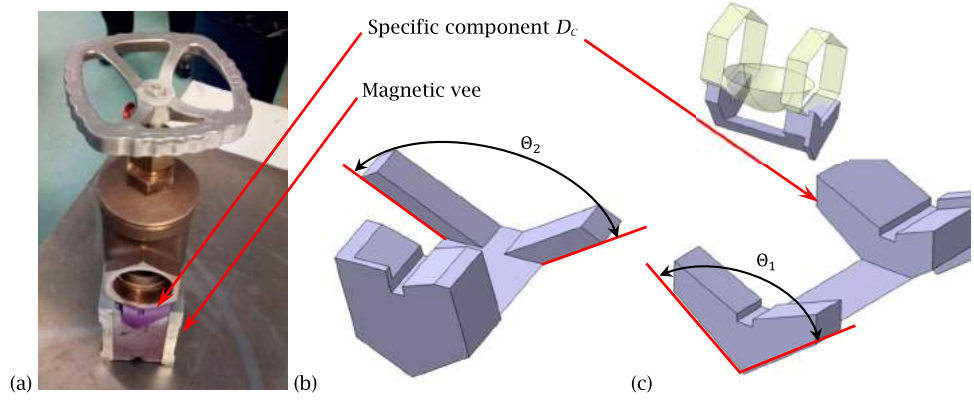

Figure 3. (a) Use of D_C to stabilize scanned objects. (b) and (c) Examples of CAD models of D_C. (c) D_C and its relative position to the housing of assembly2.

valve (see Figure 2). It is the fitting between the seal ring {Sr1} and the valve housing {H} (see Figure 2a). {Sr1} is made of polyamide and {H} is metallic (copper alloy). {Sr1} fits into a threaded area of {H} and the fitting is rather tight because some tooling is required to be able to extract {Sr1} from {H}. Consequently, {Sr1} has been removed and replaced by a 'dummy' component having an external diameter slightly smaller than that of {Sr1} to ensure an effective loose fit between this new component and {H}. Because this dummy component has a simple shape it has been 3D printed using an FDM technique (see Section 5.2 for the quantitative analysis of its dimensions).

Further, it can be stated that the quality of a scan protocol is significantly influenced by the level of interactions forces between the constitutive components of an assembly. As much as possible, this level of interaction forces must be kept as low as possible because this is reducing the use of complementary tooling during the scan protocol. Indeed, reducing the use of complementary tooling required during a scan protocol reduces the required volume around *C*, hence increasing the accessibility of the scanner, reducing the possible occlusions due to the location of the complementary tooling around *C*. Also, avoiding the use of complementary tooling reduces the needs to move *C* away from its reference position used during the scanning process, e.g., when interaction forces cannot be reached manually it can be necessary to use a vice of a more complex gripping device that requires moving *C*. Obviously, such changes of locations increase the number of registrations needed later on, hence the quality, time and complexity of the reverse engineering process.

Another consequence of the reduction of the interaction forces' intensity between components stands in the equivalence of the assembly and disassembly processes. Often, assembly/disassembly simulations are regarded as equivalent [17], i.e., inserting or extracting a component are similar tasks. Rejneri *et al.* [13] showed that disassembly processes differ from assembly ones when interaction forces between components cannot be applied on the same surfaces for the insertion or extraction phases. Such configurations appear when tooling must be used and this equipment applies unilateral forces on components (see an illustration in Figure 4). Insertion and extraction phases differ by the orientation of the corresponding forces. Therefore, reducing the intensity of interaction forces can have a significant influence on the scan protocol.

4.4. Minimizing the number of registration processes

Now, to connect the scanning protocol to an assembly or disassembly process, it is necessary to refer to the concept of assembly, resp. disassembly, sequence. Figure 2b illustrates two such disassembly sequences. In a regular scanning process, each step of the sequence would be considered as independent of the other, meaning that the reference frame could change for each of them. Consequently, a registration process using ICP-based algorithms [19] would be needed to be able to aggregate the point clouds into a common frame. Additionally, the ICP requires that the assemblies of components behave as a rigid body to be applicable. Furthermore, the transformation matrix produced by the ICP may be subjected to random sampling of the input point clouds or other optimization procedures in order to reduce its algorithmic complexity. Such an influence can be significant with respect to the accuracy of the scanner, thus avoiding the use of ICP improves the quality of the overall scans. To produce a better synergy between the scanning process and the disassembly process, we propose to look for a protocol avoiding, as much as possible, registration processes, which can reduce the scanning time, complexity, and improve the quality of the point clouds.

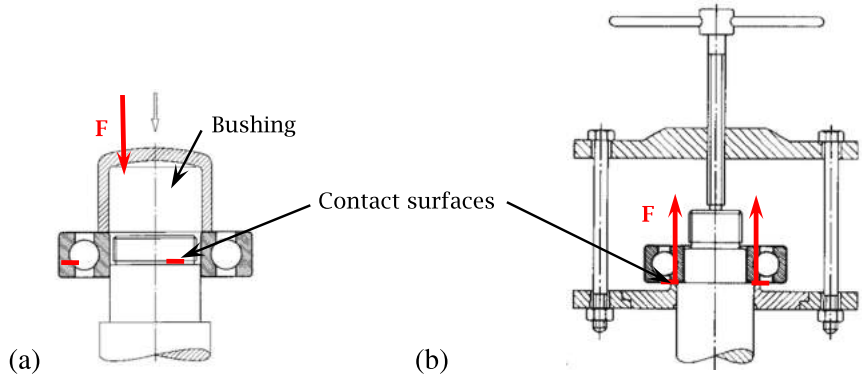

Figure 4. (a) Mounting of a ball bearing using a bushing. (b) Dismounting with a bearing puller (courtesy FAG).

To this end, it is mandatory that the reference frame (O_r, x_r, y_r, z_r) (see Figure 2a) attached to the components left after each disassembly step stands still for each of them. This property is sufficient for any assembly forming a structure, i.e., a set of components without internal mobility. In case the assembly is a mechanism, its internal degrees of freedom are as many kinematic equivalence classes that must stay immobile during each component extraction. In the example of the ball valve, it means that the reference frame (O_s, x_s, y_s, z_s) (see Figure 2a) must not move with respect to (O_r, x_r, y_r, z_r). Indeed, this is a key issue to ensure that successive point clouds acquired after every component insertion/extraction can be registered using an ICP-based algorithm. If a relative movement operates between any two kinematic equivalence classes, K_a and K_b, after they have been scanned at the i^{th} step of an assembly or disassembly sequence and (K_a , K_b) partly contribute to the point cloud of the i^{th} step, then the point cloud obtained at the $(i+1)^{th}$ step incorporates this relative movement. Consequently, an ICP-based algorithm can no longer be applied to register the i^{th} and $(i+1)^{th}$ point clouds because they don't describe the same 'rigid body'. This general statement however, can slightly be weakened if the relative movement between K_a and K_b is a rotation and the scanned area of either K_a or K_b is a surface of revolution whose axis coincides with the rotation axis of K_a with regard to K_b. In this case, the relative movement between K_a and K_b leaves the point clouds shape invariant with respect to K_a and K_b.

To illustrate the impact of such constraints, let us consider a subset of the disassembly sequence of the ball valve (see Figure 2b) with step 2 (removing {L}). During the disassembly process, components are removed sequentially. At this stage, all the components, apart from the screw {S} (already removed) and the lever {L}, must be kept in position. The result is shown on Figure 8a and it is mandatory that {N Sr1 W Sh Hc $Sr2_1$ B $Sr2_2$ H} do not move. {Sh B} form a kinematic equivalence class representing the valve axis, i.e., the degree of freedom of this mechanism. Consequently, {N Sr1 W Hc $Sr2_1$ $Sr2_2$ H} can be monitored as a whole. Controlling the position of {H} is sufficient to ensure the lack of movement of the whole set. Because {H} is mainly cylindrical and positioned on the vee, there are two degrees of freedom left, namely the rotation and the translation of {H}. Before the removal of {L}, two mechanical displacement gages are installed around the {H} as illustrated on Figure 8a. Then, when removing {L}, {H} may move slightly even though the interaction forces are kept as low as possible (see Section 4.3). After removing {L}, and to make sure that the components left have not moved, {H} is repositioned physically, if needed, to its initial position using the initial values read on the gages at an accuracy of 0.01 mm, which stands for the prescribed accuracy of this repositioning process. It is named 'mechanical registration'.

Such a protocol ensures that there is no registration needed between the scans of the ball valve with {L}, on the one hand, and without it, on the other hand (see Figure 5). Here, the protocol assumes that {Sh B} stands still because there is no mechanical gage controlling the relative position of (O_s, x_s, y_s, z_s) with respect to (O_r, x_r, y_r, z_r) under the assumption that interaction forces between {Sh B} and {N Sr1 W Hc $Sr2_1$ $Sr2_2$ H} are kept within the adherence limits (see Section 4.5).

A representative area has been selected on both scans (see Figure 5a, b) to perform the comparison of the point clouds using distance computations [4, 6]. This area is dense enough, without blending areas and well suited to reflect any rotation or translation of {H}. The point distributions necessarily differ because they result from two distinct scans. The distance computation is performed using the Hausdorff distance between the point clouds

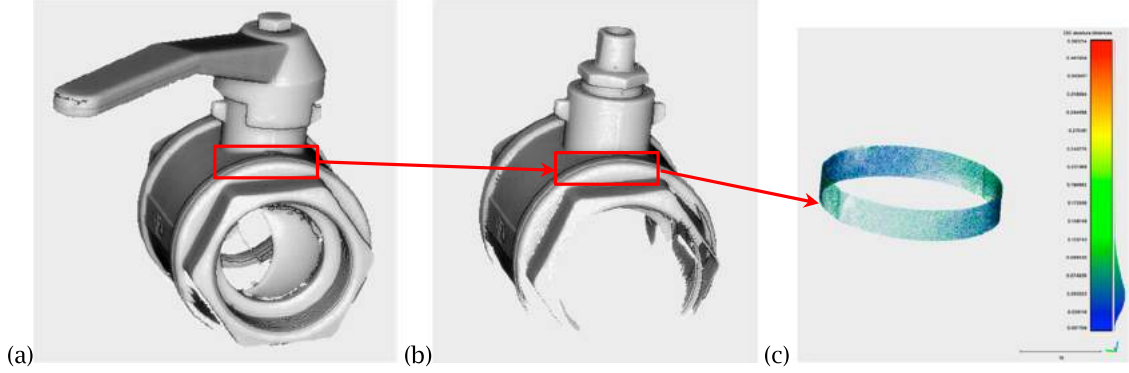

Figure 5. Point clouds comparison using CloudCompare [4]. (a) Scan of the ball valve in the 'initial' configuration prior to the disassembly process, (b) Scan after stage 2, (c) Distribution of distances between the common areas of the two point clouds (a and b). The selected areas on scans (a) and (b) are used for their comparison.

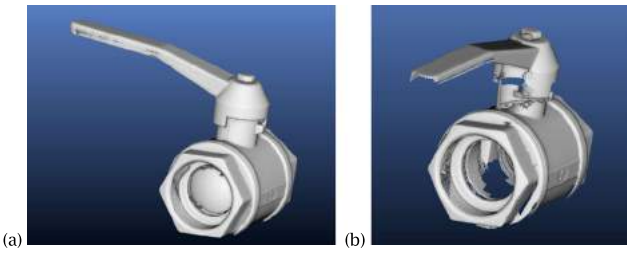

Figure 6. Scans of the ball valve after segmentation of the complementary tooling, i.e., the magnetic vee. (a) scan of the closed valve configuration, (b) scan of the open valve configuration.

and it is sensitive to their sampling, i.e., the point distribution. In addition, the distance we are looking for between the two point clouds is very small, i.e., of the order of few 0.01 mm since the repositioning of {N Sr1 W Hc $Sr2_1$ $Sr2_2$ H} is achieved with 0.01 mm accuracy. The distance computations produce an average distance of 0.06 mm with a standard deviation of 0.027 mm. When the distance computation incorporates a local least square approximation of object surfaces, which reduces the sampling effect mentioned, the avg. dist. is 0.039 mm and the std. deviation is 0.029 mm. Consequently, these two point clouds exhibit distances in the order of magnitude of the T-scan's accuracy of 0.05 mm. This justifies the fact of considering these two point clouds as registered with respect to each other.

Another interest of the registration preservation can be observed when {L} generates intermittent contacts on the housing whenever the valve is either fully opened or closed. Intermittent contacts are information hardly available in CAD assembly models where their components are set into a unique position and no information is available to characterize other key positions [14]. Here, key positions can be all scanned in (O_r, x_r, y_r, z_r) and characterize working configurations like the extreme angular positions of the ball (see Figure 6). Figures 6a and b illustrate the two corresponding scans of the closed and open configurations. These two configurations highlight the mobile kinematic equivalence class {S L Sh B} and the min and max angular positions of {L}. These two scans have been performed under the position control of {N Sr1 W Hc $Sr2_1$ $Sr2_2$ H}, i.e., no registration of these two scans is needed to characterize the fixed and mobile parts since mechanical gages have been used similarly to stage 2 of the disassembly sequence.

A common region between the two point clouds has been extracted (see Figure 7a). It is located on {H}. The distance computations produce an average distance of 0.055 mm with a standard deviation of 0.026 mm. When the distance computation incorporates a local least square approximation of object surfaces, which reduces the sampling effect mentioned, the avg. dist. is 0.03 mm and the std. deviation is 0.026 mm. Though the common area is much larger than in Figure 5, the distances obtained are fairly similar. One can observe that the largest distances are located in areas like threaded areas and blending areas, where the measurements are less accurate than in cylindrical or planar areas and the point distributions much differ. Comparing Figures 5 and 7 shows that the point distributions significantly influence the distance computation, highlighting that the distance between the positions of the real components is probably smaller than the distances obtained from the point clouds and smaller than the T-Scan's accuracy.

It is important to point out that the removal of any component or set of components, as described in Figure 2b, generates a loss of reference of this (these) component(s), i.e., their location is no longer available in (O_r, x_r, y_r, z_r), and a new reference must be created for each of them ((O_c, x_c, y_c, z_c) as an example in Figure 2a) to be able to carry on the scanning process for them. It is important for sets of components that are subjected to further assembly or disassembly operations and, in any case, it is a limitation a the 'mechanical' registration since the registration (in (O_r, x_r, y_r, z_r)) of the point clouds defined in (O_c, x_c, y_c, z_c) can be solely achieved numerically with an ICP-based algorithm.

Let *C* be the set of components taken as reference for a mechanical registration. Then, the minimum number of ICP-based registrations can be stated as follows assuming

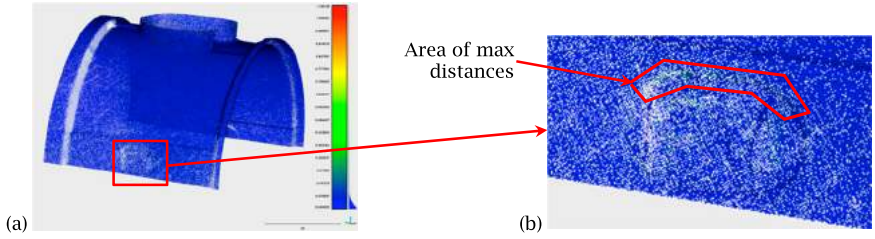

Figure 7. Point clouds comparison using CloudCompare [4]. (a) Distribution of distances between the common areas of the two point clouds (the area is a subset of the valve housing). (b) area of maximal distances located in blending areas of the housing.

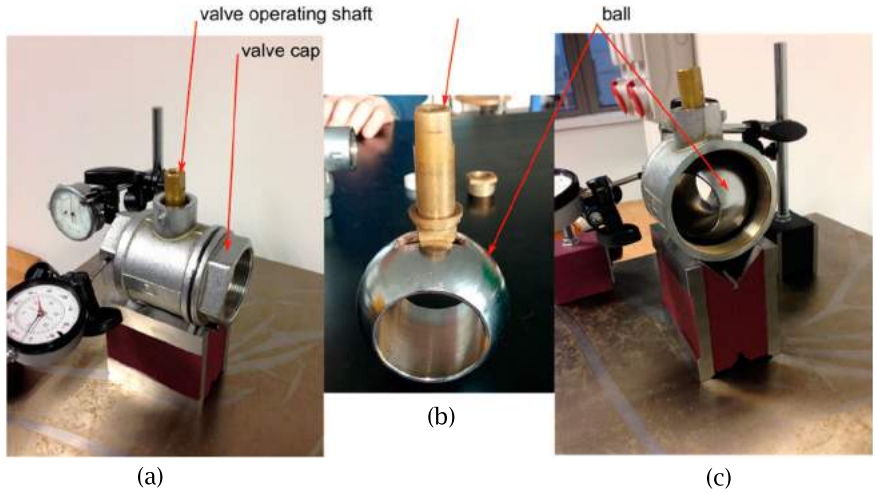

Figure 8. An example of configuration involving three hands: the removal of the valve operating shaft. The ball valve is connected to $\{Sr2_1\ Sr2_2\}$ (see Figure 2a) and to the valve cap {Hc}. Removing this shaft first requires three hands when removing the valve cap: one to hold the cap, one to hold the ball and one to hold the housing.

all subsets of components are scanned up to standalone components and a maximum number of mechanical registrations takes place:

- any extraction of a set of components C_i from C such that C_i forms a kinematic equivalence class requires an ICP-based registration to relocate the point cloud of C_i with respect to that of C;
- any extraction of a standalone component C_s from C or any C_i requires an ICP-based registration to relocate the point cloud of C_s with respect to that of either C_i or C if C_s is visible in C.

As a conclusion of this section, it can be pointed out that whenever the position of kinematic equivalence classes can be monitored with accurate sensors at each transition of an assembly or disassembly sequence, the registration process can be avoided, resulting in an improvement of the measurements' accuracy compared to [18], a quantity of information much reduced compared to [9,18], and a capability to locate more precisely movements axes between kinematic equivalence classes.

Now, comparing 'mechanical' registration with an ICP-based algorithm produces the following results. The ICP algorithm used is available from CloudCompare [4] and incorporates a random-based optimization to be able to process large point clouds. Applying it to the configuration of Figure 5, the result obtained is essentially a translation of average amplitude 0.873 mm with a standard deviation of 0.638 mm. This result shows that the ICP is also sensitive to the point distribution in the point clouds and the optimization set up to process them. As such, the 'mechanical' registration preserves the quality of the measurements.

4.5. Assembly versus disassembly sequence and number of hands

Sections 4.3 and 4.4 have referred to the concept of assembly or disassembly sequence to establish the connection with interaction forces and registration processes, respectively. Now, it is intended to address globally the concept of assembly and disassembly to set criteria helping the selection of a disassembly or assembly process and a particular sequence of such a process.

Let us consider the interaction force criterion to evaluate its impact on the selection of assembly/disassembly sequences. Additionally, let us use the test assembly2 (see Section 5.1), i.e., the gate valve. Firstly, considering the connection between the valve housing and the housing cap that operates with a seal between them (see Figure 14). The technology of this connection is not precisely known but it appears that its disassembly could not be performed without a very high level of torque, estimated around 800 Nm. Once the housing cap could be unscrewed from the housing, the torque could be reduced drastically so that the screwing movement could be operated manually. After this dismounting operation has been carried out, it has been possible to operate manually the relative movements of the other components. Secondly, the interface between the gland packing and the shaft sets another constraint, see the gland seal area circled in Figure 14c. The gland packing is a mixture of fibers and graphite grease and got deformed to produce the desired seal, making the extraction of the valve shaft manually difficult. However, the gland packing is a highly deformable material that could not be removed without severe deformations. Consequently, the scanning protocol of the gate valve has been regarded as a disassembly process.

Regarding the ball valve assembly, the scan protocol adopted is based on a disassembly sequence through the use of a dummy component to lower the intensity of the overall interaction forces between the components. Therefore, the use of an assembly process could have been used too.

A complementary issue relates to the category of deformable components in the large. Such components raise the question of their deformation or destruction and can prescribe either a disassembly-based protocol or the opposite. The latter is better suited when plastic deformations are at play because these components can be scanned at rest and after plastic deformation whereas a disassembly process requires applying a plastic deformation that cannot easily produce the rest configuration of these components.

Now, let us move to another issue about assembly sequences. Figure 2b highlights two different disassembly sequences (see the blue and red arrows for each variant). The directed graph describing the sequences exhibits also the concept of number of hands. Typically, all gray arrows illustrate steps requiring two hands, say one holding {H} or another reference component, and the other holding the removed component. However, the structure of an assembly can incorporate sequences with an arbitrary number of hands, e.g., red and blue arrows depict a step involving three hands. Anyhow, each step of a sequence is still subjected to the occlusion problem, which becomes more critical when the number of hands increases.

To this end, let us analyze the two alternatives of Figure 2b: {Hc $Sr2_1$ B $Sr2_2$ H} $\rightarrow$ {$Sr2_2$ H} + {Hc $Sr2_1$} + {B} with blue arrows and {Sh B $Sr2_2$ H} $\rightarrow$ {$Sr2_2$ H} + {Sh} + {B} with red arrows. Observing that {B} is positioned in {H} using {$Sr2_1$}, {$Sr2_2$}, and {Sh} (see Figure 4a). Though both configurations involve three hands, their major difference holds in the occlusion issue. Indeed, the 'blue' variant leaves {B} entirely occluded; hence it is not possible to acquire point clouds with a large coverage of {B} when it is in its functional position. Rather, the 'red' variant gives much better visibility to {B} and must be preferred (see Figure 9).

This analysis is also an opportunity to illustrate interactions between criteria of Sections 4.3 and 4.4. Here, {Sh B} is a kinematic equivalence class distinct from {$Sr2_2$ H} and it has been tested to not monitor with mechanical gages their relative position when removing {Hc $Sr2_1$}, considering that the interaction forces between the components were low. Only the position of {$Sr2_2$ H} has been monitored to ensure its registration at an accuracy of 0.01 mm. The comparison of the point clouds is as follows.

Figure 9b and c depict the areas used for the analysis of the registration. These areas are located on Figure 9b and named on Figure 9c. The distribution of distances produces the following results: zone A has an average distance of 0.343 mm with a standard deviation of 0.447 mm; zone B has an average distance of 0.114 mm with a standard deviation of 0.143 mm. When the distance computations incorporate a local least square approximation of object surfaces to reduce the sampling effect, in zone A the avg. dist. is 0.208 mm and the std. deviation is 0.211 mm; in zone B the avg. dist. is 0.045 mm and the std. deviation is 0.0355 mm. These results show that the distance amplitudes in zone B are rather similar to the distances obtained between the initial and final phases depicted in Section 4.4 (see Figure 5) though they are slightly increasing showing that the relocation of the valve housing could have been less accurate. Now the amplitudes in zone A are much larger, indicating that the shaft has moved.

A first explanation may hold in the clearances between {Sh} and {N Sr1 H}. Indeed, the rotational guiding of {Sh} has a radial clearance of the order 0.2 mm and {Sr1} around {Sh} does not reduce this clearance since it is a

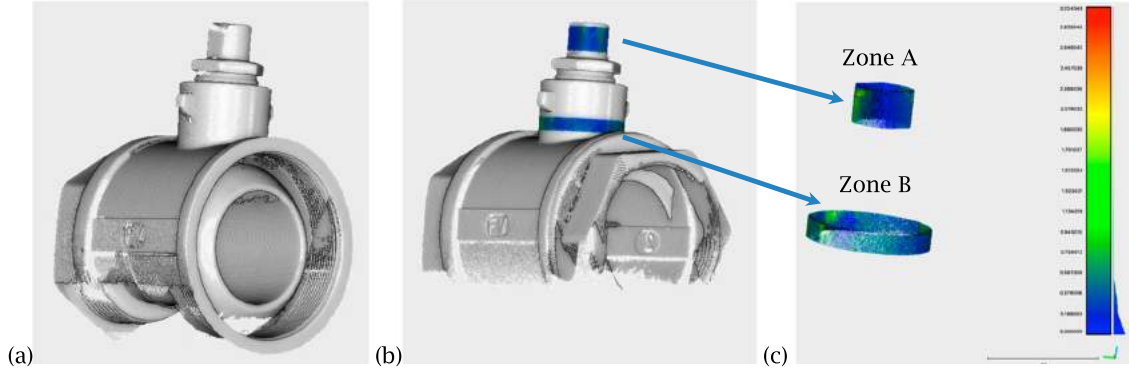

Figure 9. Point clouds comparison. (a) Scan of the ball valve after removal of {Hc $Sr2_1$}, (b) Scan before removal of {Hc $Sr2_1$} and indication of two test zones for comparison of these point clouds, (c) Distribution of distances between the common areas for the two test zones.

dummy component with a radial clearance that is difficult to monitor due to the accuracy of the 3D printer used. An alternative explanation relates to the interaction forces between {Hc $Sr2_1$} and {Sh B}. When unscrewing {Hc $Sr2_1$}, the friction between {Hc $Sr2_1$} and {B} could have created a small rotation of {B}, hence the importance of monitoring the position of the equivalence class {Sh B} with respect to {$Sr2_2$ H}.

Even though criteria of Section 4.3 have been applied, those of Section 4.4 are still prominent and those of this section have illustrated how an assembly or disassembly sequence could be selected to better fit with the scanning process.

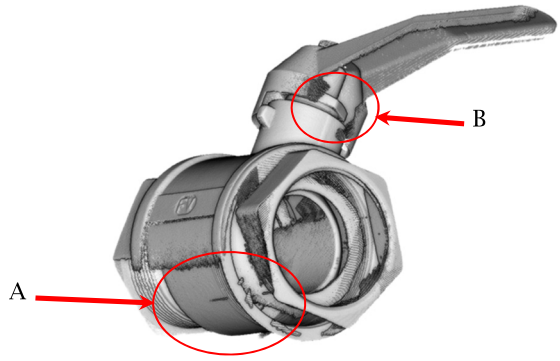

Figure 10. Merged points clouds of successive stages of disassembly operations of the ball valve with registered point clouds. Areas A and B show how the shape complementarity operates to enrich the point clouds of each component.

4.6. Reduction of occluded areas using shape complementarity

Let us now focus on the effect of point cloud accumulation obtained in synergy with an assembly or disassembly sequence. Because laser scanning faces limitations due to occluding areas and these areas originate from locally concave areas, this is recurrent problem in any scanning protocol. However, if the successive scans set up in connection with an assembly or disassembly sequence are all registered, then they can be simply accumulated, i.e., merged.

Such an operation combined with an assembly or disassembly sequence produces a synergy regarding the reduction of occluded areas. Indeed, most stages of such a sequence uncover some component areas every time a component is removed (in case of a disassembly sequence), as already illustrated in Figures 5 and 9. Such a merging process produces a point cloud M and can be used to enlarge the coverage of otherwise occluded areas and this process can be compared to the approach of Yan *et al.* [18] without requiring a large amount of data and with an improvement of the quality of the measurements since the 'mechanical' registration improves globally the measurements quality.

Figure 10 shows how concave areas, not necessarily narrow holes, can be made available across the successive scans of the disassembly sequence. Indeed, concave areas forming contacts between components become visible after the removal of one the components involved in each of these contacts. Somehow, a concave area, occluded at one step, can become a convex area later on after the removal of some component. In area A (see Figure 10), the inner cylindrical area of {H} and its common treaded area with {Hc} become digitized because they were unveiled through the removal of {Hc} and {B}. Similarly, in area B, the extremity of {Sh} common with {L} is an occluded area in {L} that becomes scanned after the removal of {L}. This refers to the shape complementarity concept and it can be extended further as follows.

If the components are scanned alone and independently of each other, their scan S_i may still contain the same occluded areas whereas the aggregation of their scan with M can still enlarge the areas covered by the scanner to produce M'. On the one hand, the shape complementarity concept shows that M' can contain a larger coverage than S_i for the corresponding component, which demonstrates the superiority of M' compared to the strict collection of S_i that cannot bring the same coverage of each component as M'. On the other hand, M brings digitized areas that can cover contact areas between components but its coverage of the component surfaces can still be improved with M', which demonstrates also the superiority of M' over M. However, it is important to recall that to be able to merge each S_i with M an ICP-based registration process must take place because components removed across the sequence loose the reference frame (O_r, x_r, y_r, z_r).

Similarly, scans of sets of components C_i (see Section 4.4) can bring similar contributions to M' under the same reasoning process.

Indeed, M' can contain interfaces between components as well as a large surface coverage of each component. Thus, M' gets closer to the point clouds produced by tomography techniques [5]. As an advantage of such a protocol over tomography, it is more accurate and it can be applied to assemblies of larger size.

More generally, the principle of shape complementarity may be used in a protocol dedicated to the scan of a standalone component C_s. Indeed, Cs enriched by its neighboring components replaces the target C_s to form a minimal assembly around C_s. This assembly can be processed as described above whenever C_s exhibits occluded areas to improve its reverse engineering.

4.7. Account for identical subsets of components

Coming back to the first stage of the disassembly sequence (see Figure 2b), its purpose is the removal of {S}, a screw. Indeed, {S} falls into a category of components designated as standard components, i.e., shape parameters and dimensions are pre-defined through standards, and few dimensional parameters are sufficient to define them completely. From this information, they can be identified entirely, even though their point cloud can contain large occluded areas in M. Segmenting M to extract such components is mandatory to be able to reverse engineer the other components. However, trying to cover the largest possible area of their boundary is not mandatory and scanning them alone to generate a S_i is not worth it. It is not necessary to scan the assembly after their removal for the same reason. All such standard components help reducing the amount of scans required and simplify the overall protocol. A first set of algorithms conforming to this approach has been developed and is illustrated in Figure 11. Consequently, the scan of {S} is not needed as well as the scan of the assembly left after its removal.

Similarly, one can perform the same observation for sets of components appearing multiple times in an assembly, i.e., occurrences of components. Such components can be easily user-identified in a real assembly and their shape property reduces to one the number of scans S_i required for each collection of occurrences. Such components fall into components belonging to a family of components, as mentioned at Section 3 and this principle can be effectively extended to such components if such families have been formalized, i.e., shape properties and driving parameters. Again, this property reduces the number scans related to the sequence of assembly or disassembly. In the case of the ball valve, either $\{Sr2_1\}$ or $\{Sr2_2\}$ need to be scanned and either the scan of {H} after the removal of $\{Sr2_2\}$ or the scan of {H} after the removal of $\{Sr2_1\}$ can be avoided. Also, the same principle can be applied to sub assemblies or sets of components having the same relative 3D positions that occur multiple times in an assembly.

Often, components or sub assemblies occurrences appear as parallel operations in an assembly or disassembly sequence. Therefore, this structural property of a sequence can be used to identify more systematically such configurations to set up and simplify a scanning protocol.

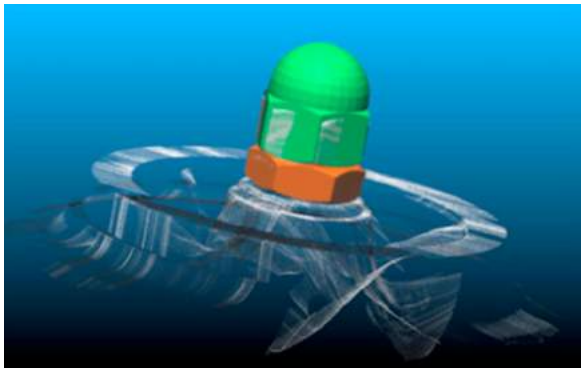

Figure 11. An example of result extracting standard components from a point cloud.

4.8. Scanning processes for components with specific morphology

The previous criteria indirectly rely on components that can be considered as rigid bodies with compact 3D volumes. To enlarge the range of components that can take part to a scan protocol, thin objects are considered because they frequently occur in industrial products. Let us focus on flat gaskets since they have a small thickness compared to the dimensions of their contours. Due to the accuracy of the scanner, it may not be possible to measure accurately their thickness but the main issue is closely related to their contour rather than their thickness, which is constant (see Figure 12).

Figure 12a depicts the raw scan of thin components; their height is close to 0.3 mm. In fact, to avoid segmentation difficulties of thin objects with respect to their planar support, the scan has been performed with the components placed on a glass sheet (2.5 mm thickness). Using this difference of material: metallic components/glass sheet, the laser beam is subjected to different refraction

(a) (b)

Figure 12. Scan results of thin components. (a) raw scans of a flat gasket and a flat check valve, (b) result after interactive extraction of the points shifted away from the surfaces of the thin components.

indices and the position of the laser spot is no longer on the glass surface, i.e., it is erroneous. The scanned glass surface is shifted further away from the real surface and, somehow, this performs a segmentation of the component lying on this surface. As a result it is possible to easily extract the point clouds of the objects, Po_i, (see Figure 12b) because the distance between these point clouds and that of the glass surface becomes much larger than the real height of the components. Then, Po_i can be processed to obtain the contours of the components.

Using a standard scanning protocol with a dry powder projected on surfaces to ensure accurate measurements would have produced a small height difference between the reference surface and the top surfaces of each component, resulting in difficulties to segment the resulting point cloud.

5. Test assemblies and analysis of their scanning protocol

5.1. Test assemblies

The proposed protocol has been tested using two different assemblies: a hydraulic ball valve (see Figure 13) (11 components) and a hydraulic gate valve (see Figure 14) (12 components). They are rather simple mechanisms, mostly with metallic components.

Consequently, the T-Scan cannot produce satisfactory results because of their specular reflectivity. To this end, a dry powder has been sprayed over the sets of components scanned to get a matt surface well suited for the T-Scan (see Figure 16b).

5.2. Analysis of scanning protocols

Here, the purpose is to complement the analyses performed throughout Section 4 that supported the description of each criterion. An illustration of the interactions between relative movements of kinematic equivalence classes, accuracy of complementary tooling, and interaction forces or clearances between components is given through their impact on measurement quality.

Let us consider the second mechanism, i.e., a hydraulic gate valve (see Figures 14 and 3a). The hand wheel operates the gate through the shaft depicted in Figure 14b, c. The purpose of the disassembly operation is the removal of the nut internal to the valve (see the location of the nut on Figure 15).

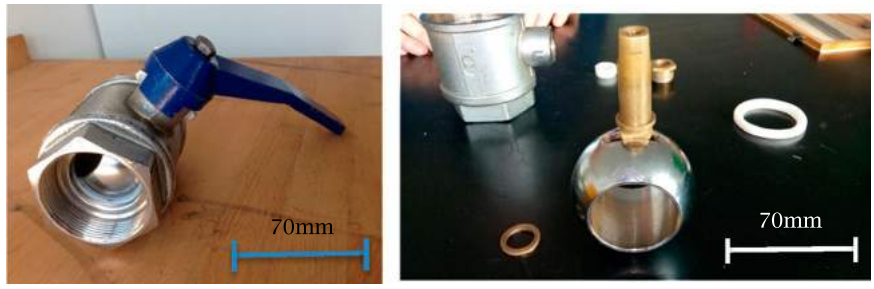

Figure 13. (a) Hydraulic ball valve assembled and (b) major components of this valve.

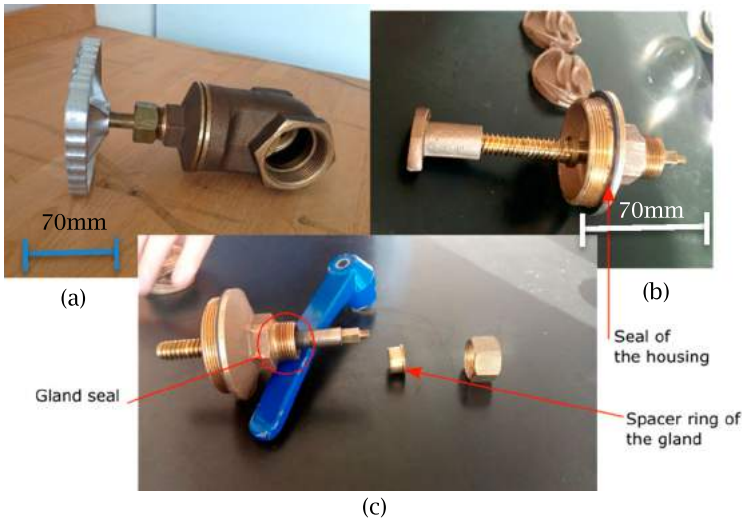

Figure 14. (a) Hydraulic gate valve assembled and (b) major components of this valve showing the seal of the housing, (c) gland seal with its spacer ring and nut placed on the housing cap.

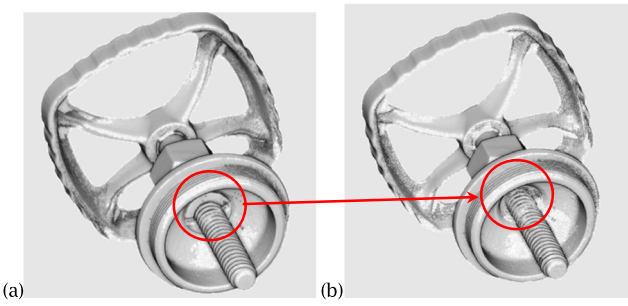

Figure 15. Point clouds comparison. (a) Scan of the gate valve sub assembly before the removal of its internal nut, (b) Scan of the previous sub assembly after the removal of the internal nut (see the difference between the circled areas).

Here, the stability requirement is handled with the use of complementary tooling (see Figure 3). The whole sub assembly gets a stable position on the vee using the dummy component depicted in Figure 3b. The scanning setup is shown in Figure 16b. Globally, the sub assembly is processed as a cylindrical part having two degrees of freedom from the isostatism standpoint. The mechanical registration has been performed with an accuracy of 0.01 mm. Then, Figure 16a gives the results of the distances computed between the scans of Figure 15a and b.

The analysis of these results produces an average distance of 0.316 mm with a standard deviation of 0.507 mm. When the distance computation incorporates a local least square approximation of object surfaces to reduce the sampling effect, the avg. dist. is 0.243 mm and the std. deviation is 0.396 mm. Now, let us analyze the distribution of these distances. Maximal deviations are located on the wheel and on the external nut of the valve where the sub assembly is supported by the dummy component. Large areas of deviation appear for distance values around 2 mm. The lessons learned from these areas show that the wheel is acting as a degree of freedom of a kinematic equivalence class in this sub-system and ought to be monitored (see Section 4.4). Figure 16b shows that this degree of freedom is not monitored with a mechanical gage. Another lesson relates to the area of the external nut that is close to the dummy component. The large deviation in this area indicates that it is connected to this dummy component. To this end, the analysis of the 3D printed dummy components has been performed to characterize their manufacturing uncertainties (see Table 1).

3D printed components have been obtained with a Makerbot Replicator 2x. As illustrated in Table 1, monitoring some key dimensions of these components leads to significant deviations compared to the nominal dimensions of the corresponding CAD model. Additionally, it has been observed that one planar surface of the 'Cap sub-Ass. Support' had significant planarity defects, though they could not be quantified easily. These values confirm that the objects used to stabilize components should be manufactured more accurately than that of the scanner, here 0.05 mm.

Table 1. Analysis of the manufacturing tolerances of dummy components and complementary tooling to stabilize components. The 'Cap sub-Ass. Support' is the component used to scan the assemblies of Figures 15, 16. Angular measures have been performed with an angle protractor of resolution 5'.

Assembly	Dummy Component	Digit. Dim	Manufact. Dim.	Δ
Ball valve	Seal ring (Fig. 2)	ϕExt: 16.42	15.97 avg.	0.45 mm
		ϕInt: 22.9	22.55 avg.	0.35 mm
		Height: 8.63	8.545 avg.	0.09 mm
Gate valve	Valve support (Fig. 3c)	Θ_1: 90°	90.25°	0.25°
Gate valve	Cap sub-Ass. Support (Fig. 3b)	Θ_2: 90°	90.5°	0.5°
Gate valve	Valve cap support	Vee angle: 90°	89.5°	0.5°

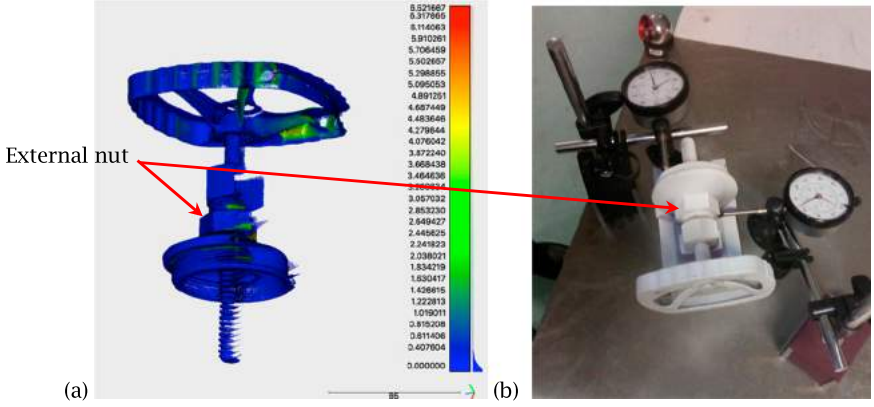

Figure 16. Point clouds comparison. (a) distribution of the distances showing significant deviations in the areas of the wheel and the external nut, (b) mechanical gages set up around the physical sub-assembly.

Table 1 content contributes to the explanation of the larger deviation between points clouds in Figure 9, where the clearance between the {Sr1} and {H} has already been identified as contributor, and in Figures 15, 16 where even larger deviations have been recorded. Consequently, 3D printing or other rapid prototyping techniques are convenient to produce dummy components, but the selected technique must lower the deviations listed in Table 1.

5.3. Synthesis of the scanning protocols

Section 4 has illustrated the principle of the proposed scanning protocol, showing its tight connection with an assembly or disassembly sequence, hence the relationship with the assembly structure since the sequence is itself connected to the assembly structure.

Criteria of scanning protocols have been described, illustrated on test examples and evaluated with respect to the accuracy of the measurements and their ability to reduce occluded areas. Combining the criteria and evaluating their impact on the real assembly helps selecting an assembly or disassembly sequence to support a scanning protocol and defining dummy components.

Then, the exploitation of the assembly or disassembly sequence forms a good reference to determine the steps where a scanning process is not required, whether it applies to a single component or a sub-assembly. In any case, reviewing the various criteria is helpful to make sure that each scan can take place with properties ensuring satisfactory measurements. The criteria and the protocol are also helpful to select and adapt the dummy components so that they correctly fit with respect to the accuracy of the scanner.

Combining scanning processes and assembly or disassembly processes has been confirmed as a synergy that generates point clouds with a larger boundary coverage than the strict collection of scans of standalone components. The point cloud obtained, *M'*, bears some comparison with the type of results produced by tomography. Here, the accuracy of the measurements is higher and the protocol can be applied to larger size assemblies than those acceptable with tomography scanners. However, the adaption of the proposed approach to large size assemblies as they can be encountered in power plants or other industries requires complementary investigations.

The interactions between criteria illustrated in Section 5.2 has revealed that a careful application of the criteria is critical to obtain good measurements and relaxing conditions like the monitoring of the relative positions of kinematic equivalence classes can be influenced by the interaction forces between components during their insertion/extraction (see also Section 4.5).

An assembly can contain a large diversity of component shapes and behaviors, some preliminary investigations have been conducted in case of flat and very thin components where laser scans can still be appropriate.

6. Conclusion

The proposed approach illustrates the interest in studying and analyzing scanning protocols so that they are able to produce more robust information that can be efficiently processed when reverse engineering assemblies. Criteria that can improve the scanning process at each step of a scanning protocol have been identified, analyzed and tested.

The synergy between the scanning protocol and an assembly or disassembly sequence has been highlighted. It is now the purpose of reverse engineering algorithms to address and adapt to this protocol to be able to exploit the points clouds obtained and determine the new software developments required to take into account the peculiarities of assembly processing. This is illustrated with the example in Figure 11 reflecting the ongoing work and in Figure 10 with the availability of the point cloud *M'*.

The proposed approach is a first formalization of a scanning protocol for assemblies as well as standalone components, to some extent, highlighting the interest of such a protocol. Further analysis and tests can be useful to extend the categories of components that can be processed and refine the criteria already identified to characterize better their interactions. Taking advantage of the content of *M'* to derive assembly constraints and a parameterization of the reverse engineered model is part of future work.

ORCID

Pablo Coves http://orcid.org/0000-0002-4886-0064
Jean-Claude Léon http://orcid.org/0000-0003-3337-081X
Damien Rohmer http://orcid.org/0000-0002-3302-5197
Raphael Marc http://orcid.org/0000-0002-1034-3408

References

[1] Angel, J.; De Chiffre, L.: Comparison on Computed Tomography using industrial items, CIRP Annals, 63, 2014, 473–476. https://doi.org/10.1016/j.cirp.2014.03.034
[2] Bernardini, F.; Rushmeier, H.: The 3D Model Acquisition Pipeline, Computer Graphics Forum, 21(2), 2002, 149–172. https://doi.org/10.1111/1467-8659.00574
[3] Brainerd, E.L.; Baier, D.B.; Gatesy, S.M.; Hedrick, T.L.; Metzger, K.A.; Gilbert, S.L.; Crisco, J.J.: X-ray reconstruction of moving morphology (XROMM): precision, accuracy and applications in comparative biomechanics research., J. Exp. Zoology., 313A, 2010, 262–279. https://doi.org/10.1002/jez.589

[4] CloudCompare: 3D point cloud and mesh processing software, http://www.cloudcompare.org, last accessed 31/03/2017.
[5] De Chiffre, L.; Carmignato, S.; Kruth, J.-P.; Schmitt, R.; Weckenmann, A.: Industrial applications of computed tomography, CIRP Annals, 63, 2014, 655–677. https://doi.org/10.1016/j.cirp.2014.05.011
[6] Girardeau-Montaut, D.; Roux, M.; Marc, R.; Thibault, G.: Change Detection on Points Cloud Data acquired with a Ground Laser Scanner, Laser Scanning 2005, ISPRS Workshop, Enschede, Netherlands, September 12–14, 2005.
[7] Heritage, G.; Hetherington, D.: Towards a protocol for laser scanning in fluvial geomorphology, Earth Surf. Process. Landforms, 32, 2007, 66–74. https://doi.org/10.1002/esp.1375
[8] Langbein, E. C.; Gao, C. H.; Mills, B. I.; Marshall, A. D.; Martin, R. R.: Topological and Geometric Beautification of Reverse Engineered Geometric Models, ACM Symposium on Solid Modeling and Applications, G. Elber, N. Patrikalakis, P. Brunet (Editors), 2004, 255–260.
[9] Li, H.; Wan, G.; Li, H.; Sharf, A.; Xu, K.; Chen, B.: Mobility Fitting using 4D RANSAC, Proc. Int. Symposium on Geometry Processing, M. Ovsjanikov and D. Panozzo Edts, Berlin, 35(5), June 2016, 79–88. http://doi.org/10.1111/cgf.12965
[10] Miura, N.; Asano, Y.: Effective acquisition protocol of terrestrial laser scanning for underwater topography in a steep mountain channel, River Research and Applications, 32, 2016, 1621–1631. https://doi.org/10.1002/rra.2986
[11] Monszpart, A.; Mellado, N.; Brostow, G. J.; Mitra, N. J.: RAPTER: Rebuilding Man-made Scenes with Regular Arrangements of Planes, Proc. ACM SIGGRAPH 2015, Los Angeles, 9–13 August 2015. https://doi.org/10.1145/2766995
[12] Natarajan, B. K.: On planning assemblies, Proc. 4th ACM Symposium on Computational Geometry, Urbana-Champain, Illinois, USA, June 06–08, 299–308, 1988. https://doi.org/10.1145/73393.73424
[13] Rejneri, N.; Léon, J.-C.; Débarbouillé, G.: Early assembly/disassembly simulation during a design process, Proc. Conf. Int. ASME, Design For Manufacturing Conference, Pittsburg, 9–12 September, 2001.
[14] Sacks, E.; Joskowicz, L.: Computational kinematic analysis of higher pairs with multiple contacts, Journal of Mechanical Design, 117, 1995. https://doi.org/10.1115/1.2826134
[15] Tucci, G.; Cini, D.; Nobile, A.: Effective 3D digitization of archeological artifacts for interactive virtual museum, Int. Archives of the Photogrammetry, Remote sensing and Spatial information sciences, 28-5/W16, 2011, 413–420.
[16] Vilmart, H.; Léon, J.-C.; Ulliana, F.: From CAD assemblies toward knowledge-based assemblies using an intrinsic knowledge-based assembly model, CAD'17 conference, Okayama, August 10–12, 2017.
[17] Wilson, R.; Latombe, J.-C.: Geometric reasoning about mechanical assembly, Artificial Intelligence, 71(2), 1994, 371–396. https://doi.org/10.1016/0004-3702(94)90048-5
[18] Yan, F.; Sharf, A.; Lin, W.; Huang, H.: Proactive 3D Scanning of inaccessible parts, ACM Trans. Graph. 33, 4, Article 157 (July 2014), 8 pages. http://doi.acm.org/10.1145/2601097.2601191
[19] Zhang, Z.: Iterative point matching for registration of free-form curves and surfaces, International Journal of Computer Vision, 13(2), 1994, 119–152. https://doi.org/10.1007/BF01427149